Metallic Impurity-Activated Crystal Growth of Boron Phosphide by Chemical Vapor Deposition and Its Physical Properties

Seiji MOTOJIMA, Yasuo MIURA, Kohzo SUGIYAMA, and Yasutaka TAKAHASHI
Department of Synthetic Chemistry, Faculty of Engineering, Gifu University, Gifu 504
(Received May 26, 1975)

Needle single crystals of boron monophosphide as large as 5—100 μm in diameter and 4 mm in length were obtained by chemical vapor deposition on an impurity painted zone of quartz substrate at 1060—1120 °C. The impurities such as Mn, Ni, Pt, Ag or Au were painted on the substrate in a form of aqueous solution of their salts and decomposed or reduced to the respective metal in hydrogen atmosphere at 1000 °C. Needle crystals with the homo p-n junction were also prepared using Ni impurity. The colors of grown crystals varied with the change of gas composition. Differences of electrical resistivity and thermoelectric power were found between the crystals of different colors.

Cubic boron monophosphide (BP, boron phosphide hereafter) has been extensively investigated during the past decade for its eminent properties as semiconductor.[1-3] Other properties of the compound, such as high melting point (about 3000 °C), high hardness (4000 kg/mm^2),[4] high oxidation resistance in air,[5] and high corrosion resistance in various chemicals,[6-8] moreover, are also interesting to use it as a high temperature material.

Single crystals of boron phosphide have been grown by direct reaction of the elements,[9] by chemical transport[10-12] and by solution growth.[13-14] Coating or epitaxial growth of the compound has been carried out by chemical vapor deposition from a gas mixture of B_2H_6–PH_3–H_2[15-17] or BCl_3–PCl_3–H_2.[18]

Needle crystals or whiskers of the compound, however, have never been obtained. It is well known that the existence of some kind of impurities accelerates the growth of whisker or needle crystals. In the present work, the growth conditions of the single crystal of boron phosphide in use of metal impurities by chemical vapor deposition from a gas mixture of boron trichloride, phosphorus trichloride, hydrogen and argon were investigated together with some physical properties of the grown crystals.

Experimental

Materials. Commercial G. R. grade phosphorus trichloride, boron carbide, and liquefied chlorine were used without further purification. Boron trichloride was prepared from boron carbide *in situ* (*vide infra*).

Preparation of Boron Phosphide. Apparatus is shown in Fig. 1. A quartz tube (7 mm o.d. and 50 mm in length), in which SiC heater was inserted, was placed at a center of reaction tube (quartz of 23 mm i.d.) as a substrate for the crystal growth. The substrate was heated at 900—1200 °C dually from outside and inside. A chlorine stream was flowed into a boron carbide bed kept at 800 °C to form boron trichloride, and the other stream of argon was bubbled through a phosphorus trichloride saturator maintained at 0 °C. The two streams were mixed at the growth zone. The surface temperature of the substrate was measured by an optical pyrometer through a window (corrected with emmision factor) and the bulk gas phase temperature by a C–A thermocouple.

Aqueous solutions of eleven compounds such as nickel acetate, hexachloroplatinic acid, tetrachloroauric acid, silver nitrate, *etc.* were painted as impurities on the substrate scratched by abrasives and decomposed or reduced to fine particles or islands of the respective metals in hydrogen atmosphere at 1000 °C.

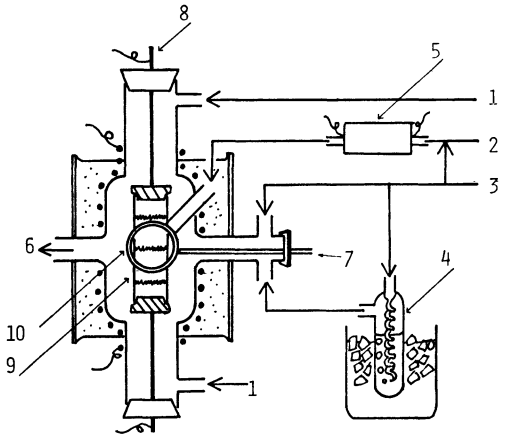

Fig. 1. The apparatus for BP growth.
(1) H_2, (2) Cl_2, (3) Ar, (4) PCl_3 saturator, (5) B_4C, (6) outlet, (7) C–A thermocouple, (8) electrode, (9) quartz substrate, (10) window.

In this paper, length of needle crystals is shown by the average length of about twenty samples selected in the order from the longest in the field of microscopy magnified by 150. Reaction time was fixed at 30 min, unless otherwise described.

Electrical Resistivity Resistivity measurements of needle crystals were performed under argon atmosphere at the temperature range of 20—120 °C using a DC wheatstone bridge (Ando Elec. Co., Model LCR-4) by conventional two probe method using a silver paste (Fujikura Chemicals, Dotite D-550) to contact the leads.

Thermoelectric Power. Crystal was bridged and attached between two copper plates (3×5 mm) separated 1 mm each other, one of which was heated by nichrome heater, where temperature difference of two edges of the crystals was measured by an iron-constantan thermocouple, and controlled in the range of 1—1.5 °C. Thermoelectric power was measured by a potentiometer.

I—V Measurements. The relationship between the current and the applied voltage (DC) was taken by a current interruptor (Hokuto Denki Co., CL-2515).

Results and Discussion

Identification of Products and Impurity Effect. In the preliminary experiment, it was found that the forms of

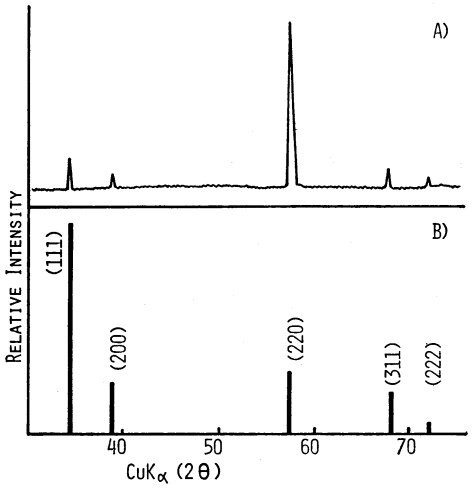

Fig. 2. X-Ray diffraction profiles.
A) BP pillar crystals set aside along the growth axis, B) BP-ASTM (No. 11—119).

deposits varied from polycrystalline coatings in the absence of nickel impurity to pillar crystals in the presence of it at 1070 °C. Although X-ray diffraction peaks of pillar crystals set aside along the growth direction shown in Fig. 2A are in good accordance with those of powder

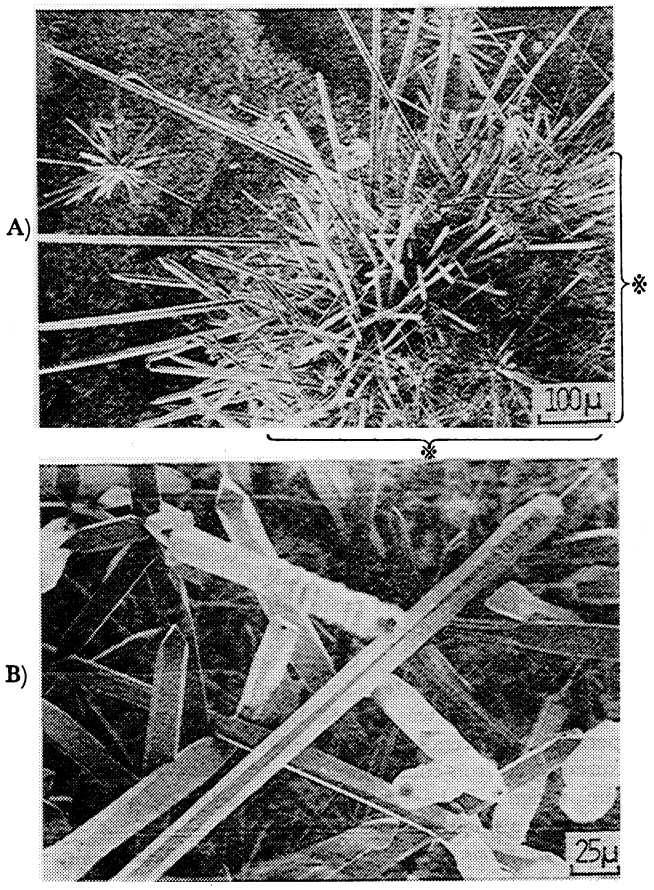

Fig. 3. Appearance of pillar crystals.
A) Pillar orange crystals, temperature: 1090 °C; reaction time; 30 min; $BCl_3/PCl_3/H_2/Ar=0.15/0.03/1.0/1.4$ (cc/s); impurity: Ni, ※ Impurity pained zone. B) Pillar black crystals, temperature: 1090 °C; reaction time: 30 min; $BCl_3/PCl_3/H_2/Ar=0.7/0.02/1.0/1.2$ (cc/s); impurity: Ni.

Table 1. Impurity effects

	Impurity (mp)	Impurity (painted forms)	Eutectic temp of binary alloy (°C) Boron-impurity	Eutectic temp of binary alloy (°C) Phosphorus-impurity	Impurity effects (crystal colors)
Fe	1535	$FeCl_3$	1149	1050	—
Co	1495	$Co(CH_3COO)_2$	1095	1023	—
Ni	1445	$Ni(CH_3COO)_2$	1080	880	++ (red and black)
Rh	1966	$RhCl_3$	1131	1300	+ (black)
Pd	1549	$PdCl_2$	845	788	—
Pt	1774	H_2PtCl_6	830	588	++ (black), + (red)
Cu	1083	$CuCl_2$	1060	714	—
Ag	960.5	$AgNO_3$		878	++ (red and black)
Au	1063	$HAuCl_4$		935	++ (red and black)
Zn	419.5	$ZnCl_2$			—
Sb	630.5	$SbCl_3$		612	—
Nd	840	$NdNO_3$			—
Cr	1890	$CrCl_3$	1550±50	1370	—
Mn	1260	$MnSO_4$		960	+ (red and black)

Reactions: conditions: Temperature; 1090 °C; reaction time, 30 min; $BCl_3/PCl_3/H_2/Ar=0.12/0.03/0.8/1.5$ (cc/s). a) (−): no or negative effects, (+): weak positive effects (below 1 mm long), (++): strong positive effects (longer than 1 mm).

data of the boron phosphide[19] (Fig. 2B), from the anomalous intensity of (110) in Fig. 2A and from the hexagonal shape (Fig. 12), it is supposed that the growth direction is ⟨111⟩, thus the side planes (110). The different growth conditions and impurities resulted in the needle or pillar crystals of different colors such as black, dark-red, and orange or yellow, while the structures and the growth directions were determined as the same as the pillar crystals grown at 1070 °C with nickel impurity described above.

When nickel impurity is painted on the substrate, pillar crystals grow only on the impurity painted zone as shown in Fig. 3A, indicating the impurity indispensable for pillar crystal growth. In Table 1, impurity effects of various metals on the pillar crystal growth at 1090 °C are summarized together with the eutectic temperatures of the relevant binary alloys.[20-22] Of the examined impurities, chromium, cobalt, iron, palladium, and copper resulted in no or negative effect on pillar crystal growth at 1090 °C, where deposition took place in a form of coatings or polygonals. On the contrary, manganese, nickel, platinum, silver, and gold indicated a positive effect at the same temperature as above, affording a straight and well-formed pillar crystal as large as 2 mm for 30 min and up to 4 mm for 90 min.

Of cource, the impurity effect varies with growth temperature. In Fig. 4, the temperature ranges of substrate for respective impurities where pillar crystal growth is possible are shown by vertical lines at the eutectic temperatures of the systems, boron–impurities. It is found that cobalt, rhodium, and iron indicate the positive effect at the higher temperature. It may be seen that

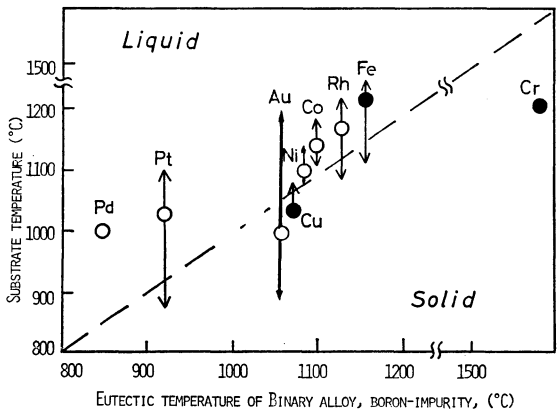

Fig. 4. Relationship between the substrate temperature and the eutectic temperature of binary alloys, boron and impurities, in BP pillar crystal growth.
(○): up to 1 mm long, (●): below 1 mm, In the case of Au impurity, the mp of Au metal it self are shown because boron is not dissolved in it.

the higher the eutectic temperature of the system of boron-impurity, the higher temperature is required for pillar crystal growth.

Hereafter nickel or platinum was used as an impurity, unless otherwise noted. The surface concentration of the impurity was fixed at *ca.* 50 μg/substrate area (cm^2) without reasons.

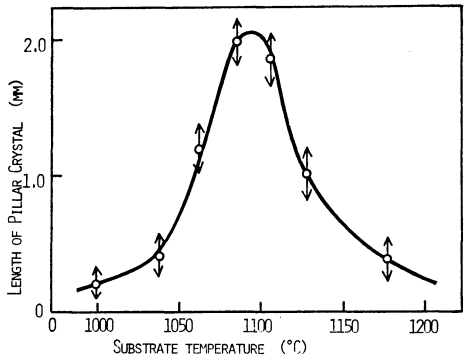

Fig. 5. Effect of substrate temperature on the length of pillar crystal.
Impurity: Pt; reaction time: 30 min; $BCl_3/PCl_3/H_2/Ar=0.05/0.023/1.3/1.25$ (cc/s).

The Effect of Substrate Temperature. The predominant factor to control the maximum length of pillar crystal is the substrate temperature. One of the results is shown in Fig. 5, where platinum was used as the impurity. An average length of 1.8—2.0 mm and the thickness of 10—50 μm was attained at 1070—1100 °C, above or below which the maximum length steeply decreased below 500 μm.

Effects of Gas Composition and Flow Rate on Pillar Crystal Growth. In the Case of Platinum Impurity: The effect of the concentration of BCl_3 and PCl_3 on the pillar crystal length is shown in Fig. 6, where total flow rate was fixed at 2.6 cc/s. According to the reaction:

$$BCl_3 + PCl_3 + 3H_2 = BP + 6HCl$$

stoichiometric ratio of $BCl_3/(BCl_3+PCl_3)$ equals to 0.5. However, the longest pillar crystal of black and hexagonal or trigonal shape was obtained between the ratios of 0.7—0.8. Woolly and faint yellow whiskers were grown at the ratio of higher than 0.95, and were determined as the mixture of boron phosphide and tridecaboron diphosphide.

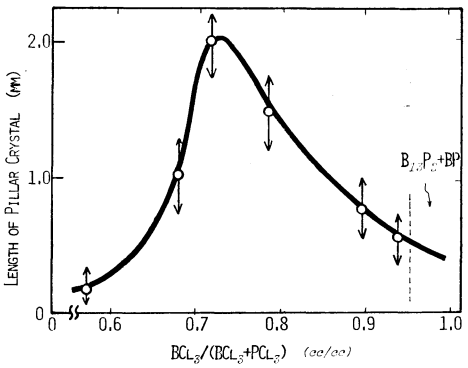

Fig. 6. Effect of the flow ratio $BCl_3/(BCl_3+PCl_3)$ on pillar crystals growth.
Impurity: Pt; reaction temperature: 1080 °C; reaction time: 30 min; H_2: 1.3 cc/s, total flow rate: 2.6 cc/s.

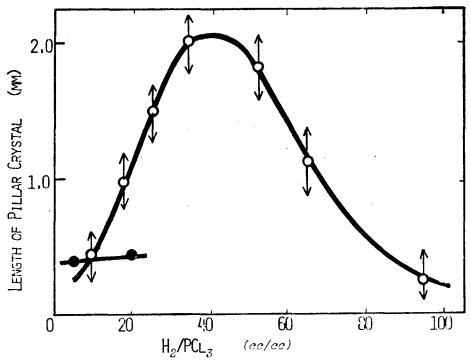

Fig. 7. Effect of the flow ratio H_2/PCl_3 on pillar crystal growth.
Impurity: Pt; reaction temperature: 1090 °C; reaction time: 30 min; $BCl_3/PCl_3=4$ (cc/cc); total flow rate: 2.4 cc/s. (○): black crystal, (●): red-orange crystal.

Phosphorus trichloride is readily reduced by hydrogen to phosphorus element. Thus the ratio of H_2/PCl_3 is expected to affect the boron phosphide crystal growth. In Fig. 7, the relationship between the length of pillar crystal and the ratio of H_2/PCl_3 in the feed stream is shown where the ratio of $BCl_3/(BCl_3+PCl_3)$ was fixed at 0.8. In spite of the dilution of phosphorus trichloride and boron trichloride by hydrogen, the length of the pillar crystal increases with the ratio up to 40, which corresponds to the phosphorus trichloride concentration of 2.5% and to the total chloride concentration of 10%. At the dilution (H_2/PCl_3) lower than twenty the color of grown crystals varied to red-orange. When the concentrations of boron trichloride, phosphorus trichloride, hydrogen, and argon calculated from the feed rates are kept at 2.0, 1.0, 50, and 47 vol %, respectively, the total flow rate to grow the longest whisker was between 2.3—3.0 cc/s which corresponds to the linear velocity of about 3 cm/s at the growth temperature of 1090 °C.

In the Case of Nickel Impurity. It was found that

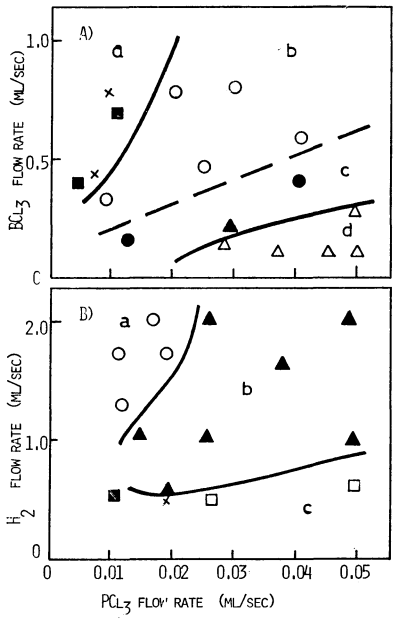

Fig. 8. Effect of relevant gas flow rates on the crystal colors and the compositions.
Impurity: Ni; (○): black pillar crystal; (●): black and orange pillar crystal; (△): orange or yellow pillar crystal; (▲): red-orange and black pillar crystal; (×): black coatings of boron and boron phosphide; (□): black coatings or brown woolly crystals of BP and $B_{13}P_2$; (■): blown and white woolly crystals of boron and boron phosphide.
A) H_2 flow rate: 1.0 cc/s, B) $BCl_3/PCl_3=0.7$ (cc/cc).

the kind of impurity affects not only morphologies of grown crystal, but also the colors of it. In Fig. 8, the distributions of the colors and the compounds of grown crystals are shown in relation with the flow rates of boron trichloride, hydrogen, and phosphorus trichloride using nickel impurity. It is found that the colors of the pillar crystals of boron phosphide vary from black of b-region to orange or faint yellow of d-region in Fig. 8A, and also from black of a-region to orange of b-region in Fig. 8B. The preferable concentration ratio of BCl_3/PCl_3 to grow the black pillar crystal of boron phosphide is about twenty, which is far rich in boron trichloride compared with the result in the case of platinum impurity, where the ratio was about three as seen from Fig. 6.

Preparation of the Crystal with Homo p-n Junction. During the CVD experiment of boron phosphide, it was found that the pillar crystal with the homo junction between the p-type black and n-type orange boron phosphide grew spontaneously by a local fluctuation of gas composition. The growth condition of the experiment was substrate temperature of 1090 °C, the gas concentration of $BCl_3/PCl_3/H_2/Ar$ of (3.7—7.4)/(1.1—1.5)/(37—38)/(55—58) vol%, and total flow rate of 2.6—2.8 cc/s in use of nickel as an impurity. The black and the orange pillar crystals are apt to grow in mixture at the part near inlets of boron trichloride and phosphorus trichloride only when nickel was used as an impurity. It was supposed that the variation of colors of pillar crystals arised from unexpected change of the ratio BCl_3/PCl_3. Thus, during the growth the inlets of boron trichloride and phosphorus trichloride was exchanged

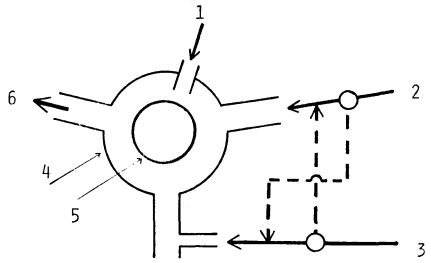

Fig. 9. Apparatus (cross section) for obtaining the pillar crystal with homo p–n junction.
1) H_2, 2) PCl_3, 3) BCl_3, 4) reaction tube, 5) quartz substrate, 6) outlet.

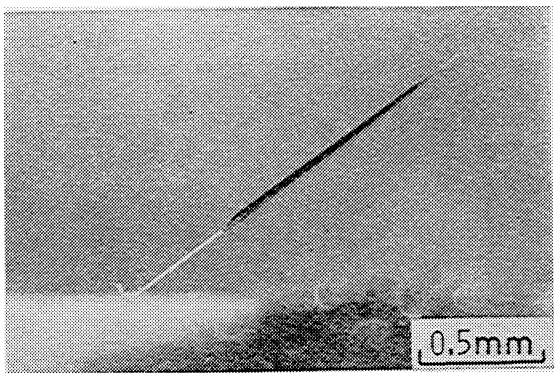

Fig. 10. Pillar crystal with homo p–n junction.
Impurity: Ni; reaction temperature: 1090 °C; reaction time; 60 min; $BCl_3/PCl_3/H_2/Ar=0.2/0.03/1.0/1.4$ (cc/s).

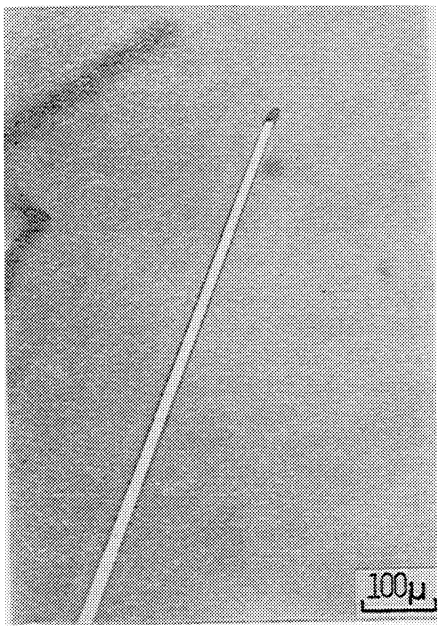

Fig. 11. Typical orange pillar crystal.
Impurity: Ni; reaction temperature: 1090 °C; reaction time: 30 min; $BCl_3/PCl_3/H_2/Ar=0.2/0.04/1.0/1.6$ (cc/s).

each other after the growth time of 30 min from the heavy lines in Fig. 9 to the dashed line, and the growth was continued for 15—30 min. The color of the pillar crystal changed from orange at the first step to black partly near tip at the second step. In Fig. 10, one of the grown crystals is shown. The black part consists of the

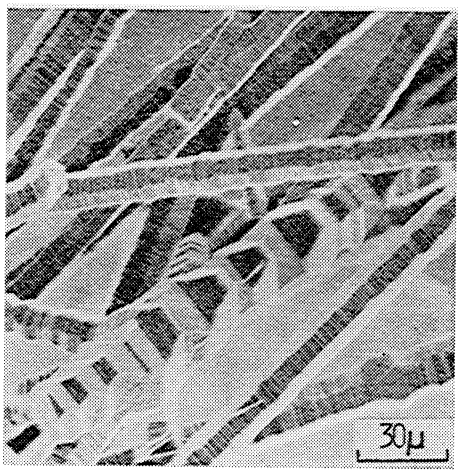

Fig. 12. Black pillar crystals with multiple growth steps on the side.
Impurity: Pt; reaction temperature: 1090 °C; reaction time: 30 min; $BCl_3/PCl_3/H_2/Ar=0.1/0.025/1.5/1.3$ (cc/s).

outer black layer and the orange core. The I–V property of the crystal will be shown later.

Crystal Morphologies and Growth Mechanism of Pillar Crystals. In contrast with the well formed red-orange crystals grown in use of nickel impurity (Fig. 11), multiple growth steps were seen frequently on the side of black pillar crystals in use of platinum impurity as shown in Fig. 12. The cross section of these crystals was commonly hexagonal- or trigonal-shaped irrespective of their colors.

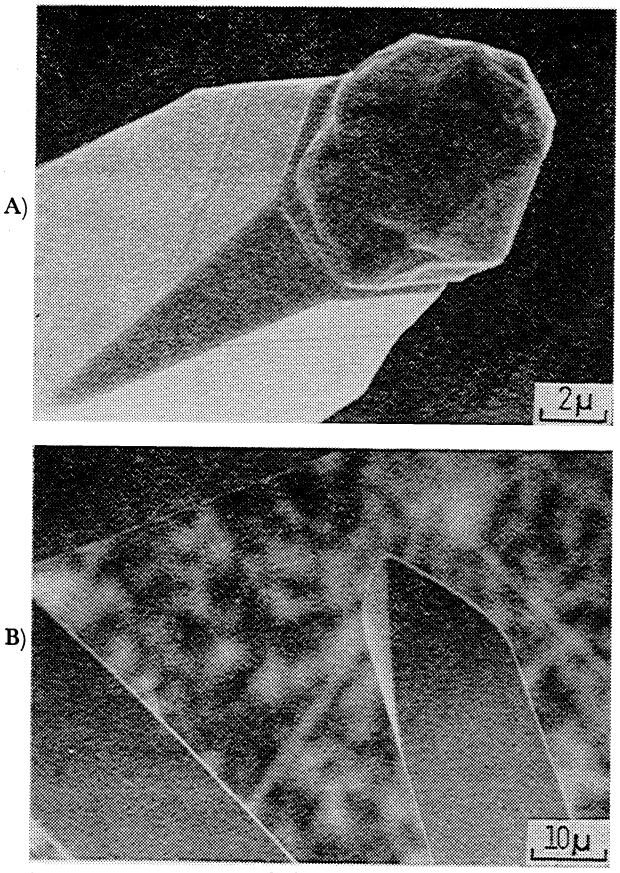

Fig. 13. The tip part of pillar crystal.
A) Orange pillar crystal, impurity: Ni.
B) Black pillar crystal, impurity: Pt.

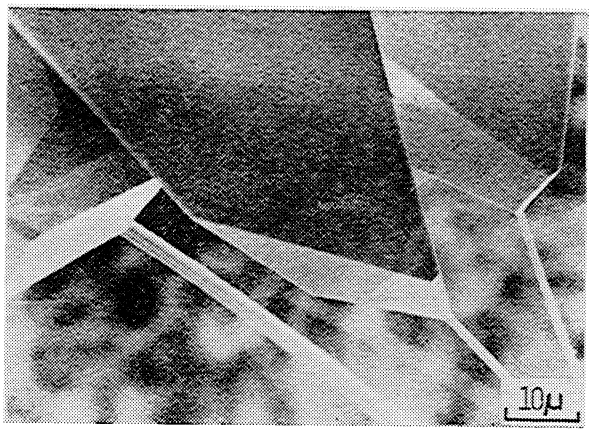

Fig. 14. Characteristic black pillar crystal grown on an orange whisker.
Impurity: Ni; reaction temperature: 1090 °C; reaction time: 30 min; $BCl_3/PCl_3/H_2/Ar=0.7/0.02/1.0/1.2$ (cc/s).

The impurities, intended to be a liquid forming agent, are indispensable for the growth of pillar crystals as described above. When nickel was used as an impurity, on the tip of the orange pillar crystal there can be seen commonly globules which may be considered to be impurity drops (Fig. 13A). On the contrary, no globules were seen on the tip of black pillar crystals irrespective of the kind of impurities (Fig. 13B). In Fig. 14, the foot part of black crystals is shown. The whole of them has yellow thin leg, from which the growth mechanism is supposed to be fast linear growth of yellow crystal by "VLS" mechanism followed by growth of black crystal by slow "VS" mechanism to the direction perpendicular to the growth axis. Unfortunately, such a double structure can be seen only when nickel was used. Thus the

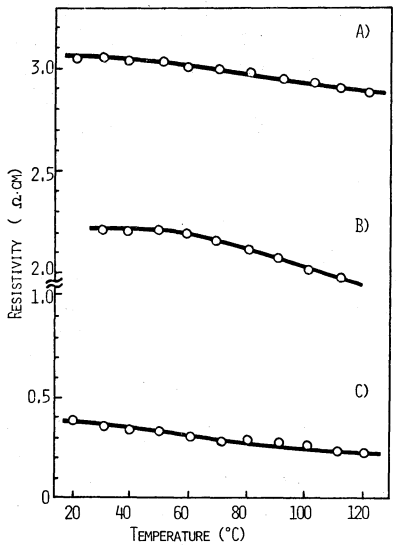

Fig. 15. Temperature dependence of electrical resistivity.
A) Impurity: Pt; $BCl_3/PCl_3/H_2/Ar=0.05/0.025/1.3/1.25$ (cc/s); black crystal.
B) Impurity: Ni; $BCl_3/PCl_3/H_2/Ar=0.3/0.035/1.0/1.45$ (cc/s); dark-red crystal.
C) Impurity: Ni; $BCl_3/PCl_3/H_2/Ar=0.12/0.03/0.8/1.5$ (cc/s); orange crystal.

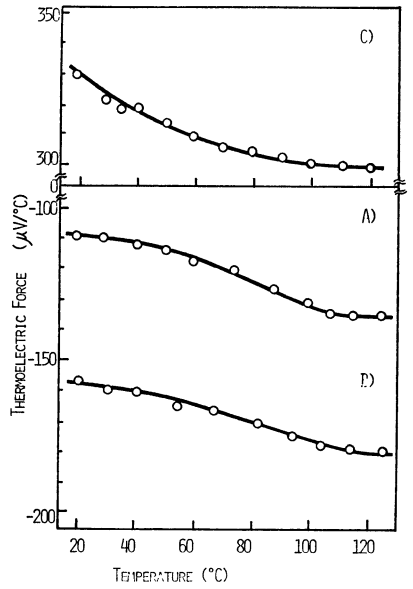

Fig. 16. Temperature dependence of thermoelectric force.

growth mechanism for other impurities than nickel remains open to further investigations.

Properties of Boron Phosphide Crystals. Electrical Resistivity: The resistivities of well-formed black, dark-red and orange or yellow crystals of hexagonal or trigonal pillars are shown in Fig. 15. These crystals were obtained in use of Pt, Ni, and Ni metal as an impurity, respectively. Although the measurements were carried out on three crystals of respective colors, the results were characteristic of respective colors within the experimental errors. Figure 15 shows that the resistivity decreases with increasing temperature, showing a characteristic semiconductor behavior. Crystal of black, dark-red, and orange have the resistivities of 3.1, 2.2, and 0.4 Ω·cm at room temperature, respectively. Chu *et al.*[12] and Nishinaga *et al.*[15] reported that the resistivities of boron phosphide were 0.5 Ω·cm (for single crystal of p-type) and 5×10^{-3} Ω·cm (for undoped layers of n-type), respectively. The resistivity of orange crystals is in good accordance with that of the former.

Thermoelectric Power. Thermoelectric powers of boron phosphide crystals of three colors, black, dark-red, and orange, are shown in Fig. 16, indicating the thermoelectric powers of −110, −160, +330 μV/°C at room temperature, respectively, and decrease with temperature. These values obtained roughly agree with the value of 240 μV/°C reported by Grinberg *et al.*[23]

Conduction types were determined as p, p, and n for crystal of black, dark-red, and orange, respectively.

Schono *et al.*[17] reported that boron phosphide of p-type and n-type was grown epitaxially on a silicon substrate at low and high flow rates of phosphine, in the reaction of phosphine, boran, and hydrogen at 950—1100 °C, respectively. Takenaka *et al.*[24] obtained a thin red-brown layer of n-type boron phosphide. From the results obtained by Schono *et al.*[17] and in present work, it is supposed that the conduction types of boron phosphide are determined by excess boron or phosphorus as p or n, respectively. Thus the transition of the growth mechanism from "VLS" (orange whisker) to

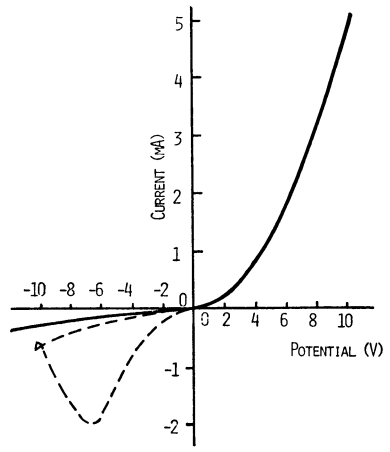

Fig. 17. I—V curve of the pillar crystal with homo p–n junction.

"VS" (black pillar) may be resulted from the solubility change of boron in impurity liquid with the whisker length because of the temperature decrease from hot surface of substrate to warm wall of reaction tube.

I—V Curve. The relationship of the applied voltage and the current of the crystal with homo p–n junction indicates a considerable rectification (Fig. 17).

References

1) C. C. Wang, M. Cardona, and A. G. Fischer, *RCA Rev.*, **25**, 159 (1964).
2) R. J. Archer, R. Y. Koyama, E. E. Loebner, and R. C. Lucas, *Phys. Rev. Lett.*, **12**, 538 (1964).
3) B. Stone and D. Hill, *Phys. Rev. Lett.*, **6**, 282 (1960).
4) V. I. Matkovich, *J. Amer. Chem. Soc.*, **83**, 1804 (1961).
5) R. C. Vickery, *Nature*, **184**, Suppl. No. 5, 268 (1959). (*Chem. Abstr.*, **54**, 7392 (1960)).
6) F. V. Williams and R. A. Rueherwein, *J. Amer. Chem. Soc.*, **82**, 1330 (1960).
7) J. Cueilleron and F. Thevenot, *Bull. Soc. Chem. Fr.*, **1965**, 402. (*Chem. Abstr.*, **62**, 14164 (1965)).
8) I. Yu. Andreeva and G. V. Efremov, *Vestn. Leningr. Univ. Ser. Fiz. i Khim.*, **19**, No. 2, 130 (1964).
9) K. P. Ananthanarayanan, C. Mothanty, and P. J. Gielisse, *J. Cryst. Growth*, **20**, 63 (1973).
10) Z. S. Medvedeva, J. H. Greenberg, E. G. Zukov, and N. P. Lužnaja, *Kristall Technick*, **2**, 523 (1967).
11) Z. S. Medvedeva, J. H. Greenberg, and E. G. Zukov, *ibid.*, **4**, 487 (1969).
12) T. L. Chu, J. M. Jackson, and R. K. Smeltzer, *J. Cryst. Growth*, **15**, 254 (1972).
13) B. V. Baranov, Ya. A. Oksman, V. D. Prochukhan, and V. N. Smirnov, *Opt. Spectrosk.*, **19**, 987 (1965).
14) T. L. Chu, J. M. Jackson, and R. K. Smeltzer, *J. Electrochem. Soc.*, **120**, 802 (1973).
15) T. Nishinaga, H. Ogawa, H. Watanabe, and T. Arizumi, *J. Cryst. Growth*, **13/14**, 346 (1972).
16) T. L. Chu, J. M. Jackson, A. F. Hyslop, and S. C. Chu, *J. Appl. Phys.*, **42**, 420 (1971).
17) K. Schono, M. Takigawa, and T. Nakada, *J. Cryst. Growth*, **24/25**, 193 (1974).
18) J. Lindström, K. Fundell, and A. Lind, "Proceedings of the 4th International Conference on CVD (1973)," Electrochem. Soc. (1973), p. 546.
19) J. A. Perri, S. Laplaca, and B. Post, *Acta Crystallogr.*, **11**, 310 (1958).

20) M. Hansen and K. Anderco, "Constitution of Binary Alloys," McGraw-Hill, New York, Toronto, London (1958).
21) R. P. Elliot, *ibid.*, First Supplement (1964).
22) F. A. Schunk, *ibid.*, Second Supplement (1969).
23) Ya. Kh. Grinberg, Z. S. Medvedva, A. A. Elisseve, and E. G. Zhukov, *Doklady*, **160**, 337 (1965).
24) T. Takenaka, M. Takigawa, and K. Schono, *Japan J. Appl. Phys.*, **14**, 579 (1975).